Using electrical impedance tomography for rapid determination of starch and soluble sugar contents in Rosa hybrida

Ji Qian (qianji167@163.com)
Hebei Agricultural University https://orcid.org/0000-0003-3782-2967
Juan Zhou
Hebei Agricultural University
Bao Di
Hebei Agricultural University
Yang Liu
Hebei Software Institute
Gang Zhang
Hebei Agricultural University

Research

Keywords: EIT, reconstructed boundary voltage value, soluble sugar content, starch, regression model

Posted Date: May 13th, 2020

DOI: https://doi.org/10.21203/rs.3.rs-27619/v1

Version of Record: A version of this preprint was published at Scientific Reports on February 3rd, 2021.
See the published version at https://doi.org/10.1038/s41598-021-82456-1.

Abstract

Background

Soluble sugar and starch, as carbon sources, directly participate in plant metabolism by providing energy. Conventional determination of plant starch and soluble sugar content usually involves destructive sampling, complicated procedures, and considerable amounts of chemicals and labor. Therefore, there is an urgent need to develop a non-destructive and rapid method for determining plant starch and soluble sugar contents. Electrical impedance tomography (EIT) technology has been used to determine the physiological state and cold resistance of plant tissues. However, so far there have been no reports on the use of EIT for the rapid estimation of soluble sugar and starch contents.

Results

In this study, EIT was used to obtain reconstructed voltage values and estimate starch and soluble sugar contents in the stems of three *Rosa hybrida* cultivars during February to May. Stems from two of the cultivars were used for establishing regression models for starch and soluble sugar contents as functions of reconstructed voltage values. The third cultivar was used to test the accuracy of the regression models. The results showed that the reconstructed voltage value significantly correlated with soluble sugar and starch contents. The quadratic regression model was best for determining soluble sugar content and the logarithmic regression model was best for determining starch content.

Conclusions

Thus, we preliminarily established and verified regression models for estimating soluble sugar and starch contents using reconstructed voltage values of rose stems. These data provide technical support for using EIT to analyze changes in physiological parameters and to rapidly estimate physiological indexes of plants.

1. Background

Soluble sugar and starch, the photosynthetic products of higher plants, are the main substances produced through plant carbon metabolism via the Calvin cycle and play an important role in osmotic adjustment. To a certain extent, changes in soluble sugar content reflect the adaptability of a plant to environment change [1–4]. Wang et al. (2016) showed that during the dehardening period, as the temperature naturally changed, the soluble sugar content in rose plants decreased and the starch content increased [5]. At present, starch content and soluble sugar content are usually determined using colorimetric approaches. Colorimetric approaches are easily affected by the amount of chromogenic agents, proportion of different carbohydrates in the plant, and the experimental procedures and optimized [6–8], there are still shortcomings of

such methods. These shortcomings include destructive sampling, extensive use of chemicals, complicated procedures, and errors caused by human operation. Therefore, it is urgent to develop a non-destructive and rapid method for determining starch and soluble sugar contents in plants.

In 1976, Swanson from the Wisconsin Madison University in the United States, first proposed the use of electrical impedance tomography (EIT), which has since attracted extensive attention. The EIT system can quickly and efficiently detect changes in the electrical characteristics of an organism, which are associated with changes in physiological state. The voltage and current across sections of the subject are measured at the surface and the internal conductivity distribution is reconstructed. To do this, a set of EIT sensors are attached around the surface of the object of study and an electric signal with an alternating current of constant amplitude is applied to the object. An electrical instrument connected to the sensors is used to measure the boundary voltage, which is then processed and output as an intuitive two-dimensional color image [9–12].

EIT is mainly used in animal experiments and tentatively in human clinical research related to digestive, respiratory, and craniocerebral issues [13–17]. In recent years, some researchers have used EIT technology to study soil properties, wood decay, root physiological state, and cold resistance of plants [18–22]. There are few reports on the establishment of regression models for the effect of plant physiological state on EIT parameters. EIT technology can show that the impedance changes with frequency inside the object and be used to display an image of the functional state of an organ undergoing physiological changes [23]. The rapid and non-destructive determination of plant starch and soluble sugar contents can be achieved through the following procedure: the excitation signal is loaded to the object by selecting suitable electrodes; the surface voltage is detected; data are collected and processed; the image is reconstructed using algorithms; and the corresponding two-dimensional color image is displayed on a computer.

We hypothesized that the starch and soluble sugar contents in plant cells and tissues would change during the dehardening period. The resulting differences in electrical conductivity could be detected using EIT technology by measuring the boundary voltage. Hence, the dynamics of the soluble sugar and starch contents could be detected. The objective of this study was to utilize the EIT imaging technology to establish regression models for the starch and soluble sugar contents as functions of reconstructed EIT boundary voltage values using data from two floribunda rose (*Rosa hybrida*) cultivars. The accuracy of the models was tested using a third floribunda rose cultivar. This study provides a technical and theoretical basis, and a mathematical model, for the rapid and non-destructive determination of starch and soluble sugar contents in plants.

2. Results

2.1 EIT images and their reconstructed boundary voltage values

One EIT image was selected from each of the three rose cultivars at different temperatures at each sampling time (Fig. 1). During the period of external temperature change, the EIT image accurately displayed the location, shape, and size of the rose stem as well as the distribution of resistivity. The darker the blue color, the smaller the resistivity and the corresponding reconstructed boundary voltage value. In EIT images, the pure blue color corresponds to the maximum value of the reconstructed result. Over the course of the dehardening period, the blue parts of the EIT images of the stems of the three rose cultivars gradually darkened. Figure 2 shows the change of the reconstructed EIT boundary voltage value of the stems of the three rose cultivars during the dehardening period. As shown in Fig. 2, the reconstructed boundary voltage values of the stems of the three rose cultivars showed a significant downward trend. The slopes of the curves of 'Red Cap', 'Tender and Soft as Water', and 'Carefree Wonder' were − 8.84, -8.89, and − 0.92 respectively. Of these, the downward trend of 'Carefree Wonder' was the most significant and the reconstructed boundary voltage value of 'Carefree Wonder' was between 0.078 and 0.036 (Fig. 1). There were no significant differences in the reconstructed boundary voltage values between the three cultivars ($P < 0.05$).

2.2 Changes in soluble sugar and starch contents

During the dehardening period, the soluble sugar content in the stems of the three rose cultivars showed an overall downward trend. The soluble sugar contents all increased slightly on April 25, and then continuously decreased, with the lowest values observed on May 16 when the last sampling was performed (Fig. 3A). The soluble sugar contents of each of the three rose cultivars were significantly lower on May 16 than at the other four sampling times ($P < 0.01$). The soluble sugar contents of 'Red Cap', 'Tender and Soft as Water', and 'Carefree Wonder' on May 16 were 41.99%, 45.38%, and 41.35% lower, respectively, than on February 22. However, there were no significant differences in the soluble sugar contents of the same cultivar between the March 14, April 4, and April 25 samples. Furthermore, there were no significant differences in the soluble sugar contents of the different cultivars at each sampling time.

During the dehardening period, the starch content of the stems of all three rose cultivars showed an increasing trend (Fig. 3B). The overall rate of increase in starch content of 'Carefree Wonder' was higher than that of the other two cultivars. The starch content of all three cultivars obviously increased during the period from February 22 to March 14, but the rate of increase was lower for the rest of the sampling period. The starch content of all three cultivars was significantly higher on May 16 than on the four other sampling dates ($P < 0.05$). The starch contents in the stems of 'Red Cap', 'Tender and Soft as Water', and 'Carefree Wonder' were 41.42%, 44.51%, and 58.93% higher on May 16 than on February 22. The starch content of the stem of 'Carefree Wonder' significantly differed between the five sampling times ($P < 0.05$). The starch contents of 'Red Cap' and 'Tender and Soft as Water' significantly differed between February 22 and the four other sampling times ($P < 0.05$); there were no significant differences in sugar content between those four sampling times. There was no significant difference in the starch content between different cultivars at each sampling time.

2.3 Establishment of the regression models for starch and soluble sugar contents as functions of reconstructed EIT boundary voltage values

The soluble sugar and starch contents and the corresponding reconstructed EIT boundary voltage values of the two cultivars 'Red Cap' and 'Carefree Wonder' were used to establish a regression model. The measured EIT boundary voltage values ranged from 0.036 to 0.089. These values were 100 times smaller than the values of starch and soluble sugar contents. Therefore, the measured boundary voltage values were multiplied by 100. These amplified values were used together with the soluble sugar and starch contents in linear and nonlinear regression analyses. The regression model with the greatest R^2 was preferentially selected as the best model. The results are shown in Table 1. The R^2 values of the established linear, logarithmic, and quadratic regression models for soluble sugar content as a function of reconstructed EIT boundary voltage value, were 0.863, 0.811, and 0.897, respectively ($P < 0.001$). Thus, for soluble sugar, the quadratic regression model had the greatest R^2. The R^2 values of the established linear, logarithmic, and quadratic regression models for the starch content as a function of reconstructed EIT boundary voltage value, were 0.894, 0.959, and 0.935, respectively ($P < 0.001$). Thus, for starch, the logarithmic regression model had the greatest R^2.

Table 1
Analysis of the regression for soluble sugar and starch contents as functions of reconstructed electrical impedance tomography (EIT) boundary voltage values

Item	Index	Equation	Regression model	R^2	F
Soluble sugar value	Boundary voltage reconstruction value	Linear	$y = 0.868x + 2.125$	0.863	50.527
		Logarithmic	$y = 4.758\ln(x) - 1.034$	0.811	34.411
		Quadratic	$y = 0.142x^2 - 0.823x + 6.757$	0.897	30.538
Starch value	Boundary voltage reconstruction value	Linear	$y = -0.333x + 5.271$	0.894	67.350
		Logarithmic	$y = -1.917\ln(x) + 6.634$	0.959	104.964
		Quadratic	$y = 0.059x^2 - 1.032x + 7.189$	0.935	50.132

2.4 Testing the accuracy of the regression models for soluble sugar and starch contents as functions of reconstructed EIT boundary voltage values

The measured data from the cultivar 'Tender and Soft as Water' was used to test the accuracy of the regression models. The Root Mean Square Error (*RMSE*), Relative Error (*RE*), *Offset*, and the coefficient of determination (R^2) of the fitted linear regression based on measured and predicted values were [illegible] quadratic models. The *RE* is the percentage of

the absolute error of the measurement divided by the measured value. Generally, the *RE* can well reflect the reliability of a measurement and was calculated using the Eq. 3. *RMSE* is used to estimate the deviation between the predicted value and the measured value [24], and is usually used as a standard for assessing the predicted results of a model. The *RMSE* was calculated using Eq. 4.

$$RE = \frac{\sum_{i=1}^{n} f(x_i) - \sum_{i=1}^{n} y_i}{\sum_{i=1}^{n} y_i} \times 100\% \qquad (3)$$

$$RMSE = \sqrt{\frac{1}{n}\sum_{i=1}^{n}\left(f(x_i) - y_i\right)^2} \qquad (4)$$

where x_i refers to the measured reconstructed EIT voltage values of 'Tender and Soft as Water'; $f(x_i)$ is the soluble sugar content and starch content calculated by the model; y_i is the measured value of soluble sugar and starch content corresponding to x_i; and $n = 5$ represents the five sampling times within the dehardening period.

The validation result of the models is shown in Table 2. The quadratic regression model for soluble sugar content prediction ($y = 0.142x^2 - 0.823x + 6.757$) had the greatest R^2 (0.897), and the smallest *RMSE* (0.811), *RE* (10.64%), and *Offset* (1.38). Therefore, it was the best model and the prediction accuracy was 89.36%. The logarithmic regression model for starch content prediction ($y = -1.917\ln(x) + 6.634$) had the greatest R^2 (0.959) and R^2 (0.948), and the smallest *Offset* (0.022). The *RMSE* was only 0.010 times greater than that of the linear model. Taking into consideration the R^2, *RMSE*, *RE*, *Offset*, and $R^{\prime 2}$, the logarithmic model was the best model for predicting starch content, with a prediction accuracy of 93.98%.

Table 2
Indexes for assessing the fitting of measured and predicted values of soluble sugar and starch contents

Item	Index	Regression model	*RMSE*	*RE* (%)	*Offset*	R^2
Soluble sugar	Boundary voltage	$y = 0.868x + 2.125$	1.060	11.56%	3.294	0.923
		$y = 4.758\ln(x) - 1.034$	1.197	11.26%	4.293	0.876
		$y = 0.142x^2 - 0.823x + 6.757$	0.811	10.64%	1.380	0.977
Starch	Boundary voltage	$y = -0.333x + 5.271$	0.202	−5.58%	0.554	0.926
		$y = -1.917\ln(x) + 6.634$	0.212	−6.02%	0.022	0.948
		$y = 0.059x^2 - 1.032x + 7.189$	0.257	−5.88%	0.861	0.824

3. Discussion

Carbohydrates, which exist mainly as starch and soluble sugar, are the basic substances that directly participate in plant metabolism by providing energy and carbon sources. Thus, they are the important indicators of the intensity of life activities in plants. Many studies have shown that carbohydrates can also act as signaling molecules, connecting with hormone and nitrogen signals to form a complex signaling network. Thus, carbohydrates participate in the regulation of a series of plant metabolic activities. Carbohydrate content in plants directly affects plant growth and ecological adaptability [25–28]. In the present study, it could be seen that during the dehardening period, large amounts of soluble sugar were used for growth and the content of soluble sugar in the rose stems showed a decreasing trend. As the environmental temperature and duration of sunshine increases, more photosynthetic products are produced by new green leaves [22, 29]. Meanwhile, the activities of various enzymes involved in photosynthesis are enhanced. As a result, the starch content in the stem increases, as was observed in the present study. Therefore, the content of soluble sugar and starch in the plant changes with the temperature of the external environment.

EIT technology uses the electromagnetic characteristics of a tissue to reconstruct the distribution of resistivity inside the tissue and display these changes as an image. The interaction of charged ions and ionic groups allows biological tissues to maintain a certain structure and function. Changes in physiological state result in changes to the electrical characteristics, which can be sensitively captured by the EIT system. Therefore, EIT is an imaging technology that can reflect the internal structure and function of tissues and organs. In response to changes in the external environment, plants present a series of noticeable changes, such as in plasma membrane permeability, intracellular solutes, and cell growth and differentiation [30]. In the present study, the stem segment was exposed to the EIT saline solution for only 30 s, so the effect of the water content on the rose stem boundary voltage could be ignored

Rose stems mainly possess fiber wood-related characteristics, which were affected by the changes in physiological parameters and in turn led to the changes in the stem dielectric properties. These dielectric changes caused differences in the reconstructed boundary voltage values. Rose stems are composed of a large number of cells of different shapes. The cells have high impedance to low frequency currents (f < 1 kHz) that only flow in the extracellular space [31]. In the present study, we used 1 kHz excitation currents. The majority of the current flows only in the extracellular spaces, and only a small part of the current passes through the cell membrane into the cell. Therefore, the extracellular impedance and part of the intracellular impedance affected the reconstructed EIT boundary voltage value.

Soluble sugar dissolves in the cell fluid, while starch is insoluble in water. As the environmental temperature gradually increases, the carbohydrates in the stem change accordingly. In the present study, the soluble sugar content gradually decreased while the starch content gradually increased. This affected the flow of the electric current. As a result, the stem resistivity and the reconstructed EIT boundary voltage value decreased over the course of the dehardening period. It was found that the soluble sugar and starch contents correlated well with the reconstructed EIT boundary voltage value. The R^2 of the best regression models for predicting soluble sugar content and for predicting starch content were 0.897 and 0.959, respectively ($P < 0.001$). In addition, by using rose stem samples from a third cultivar for testing, both of the models were found to have decent accuracy. Therefore, it will be possible to use the reconstructed EIT boundary voltage value to predict plant soluble sugar and starch contents as a substitute for cumbersome chemical methods.

4. Conclusions

The rapid advancement of EIT technology deems it feasible for use as a rapid and non-destructive method for the determination of physiological parameters of plants. In this study, the mathematical models for estimating soluble sugar and starch contents were preliminarily explored using the reconstructed EIT boundary voltage value of rose stems. The results provide theoretical and technical basis for the application of EIT technology in the rapid analysis of the physiological parameters of plants and their changes. This study may also promote the application of EIT technology for physiological studies of plant resistance.

5. Methods

5.1 Rose plants, growth conditions, and sampling

The biennial floribunda rose (*R. hybrida*) cultivars 'Red Cap', 'Tender and Soft as Water', and 'Carefree Wonder', which were grown in the Specimen Park (38°50' N, 115°26' E) of Hebei Agricultural University, Baoding City, Hebei Province, China, were used in the study. A completely randomized block design was adopted. Before the roses were planted, the soil was ploughed and barnyard manure fertilizer was applied. After planting, the soil was watered one to two times per week according to rainfall conditions. 25 m × 0.30 m between plants. There were five

replicate plots for each cultivar. A total of 450 plants were grown (30 plants/plot × 5 replicates × 3 cultivars = 450 plants). Management was applied to maintain consistent growth of the different rose cultivars. During the dehardening period from February to May 2016, the plants were sampled every 20 days and five times in total. During the sampling period, the environmental temperature was recorded by the meteorological station in the Specimen Park of Hebei Agricultural University. The daily average temperatures of the five sampling days were 1.45 °C, 7.7 °C, 13.65 °C, 19.65 °C, and 18.75 °C (Fig. 4).

Eight plants with a decent growth state were selected from each cultivar. Three to four branches (1 cm diameter) with leaves, from the middle of each plant, were sampled. The samples were washed three times with tap water and a further three times with deionized water. The water on the surface of the samples was removed with absorbent papers. A part of each sample was stored in a refrigerator at 4 °C for 2 h and then used in the EIT measurement. The other part of each sample was oven dried for the conventional determination of starch and soluble sugar contents.

5.2 Determination of reconstructed EIT boundary voltage value

In this study, we used the relatively high precision EIT system that was independently developed by researchers from the Fourth Military Medical University, Xi'an City, Shaanxi Province, China. We referred to the methods they used in animal or human cardiopulmonary and craniocerebral studies [32]. The diameters of the rose stem segments were much smaller than those of animal organs. Therefore, a number of preliminary tests were conducted in order to find the excitation current that provided the best imaging and avoided noise interference. The chosen excitation current for the EIT system in this study was 1 kHz and 250 μA. A cylindrical perspex container with an inner diameter of 160 mm was filled with 0.9% physiological saline solution (impedance does not change with frequency). Sixteen electrodes of 10 mm diameter were equidistantly installed on the wall inside the container. The electrode plane was 25 mm from the bottom of the container and 10 mm below the surface of the physiological saline solution. Stem segments that were 70–90 mm long and less than 4 mm in diameter (excessively thin segments downgraded the image quality) with even thickness and growth status were selected. The stem segments were inserted vertically in the container, 20 mm away from the wall. After the surface of the saline solution became still, 10 EIT images were taken. Of these, the image with the least noise interference was selected and the corresponding reconstructed boundary voltage value was used as the final datum.

The entire data acquisition process took only 30 s. In such a short time, the effect of the saline solution on the stem segment and the subsequent effect on the precision of the image could be ignored. In order to obtain the best quality image, we used the frequency-difference (FD) based quasi-static imaging algorithm and the weighted frequency-difference and damped least-squares (WFD-DLS) based EIT algorithm to reconstruct the image. The weighted frequency-difference method was used for data processing, which eliminated the influence of background noise on the imaging quality. Meanwhile, the

regularization method combined with the damped least-square reconstruction algorithm was used to deal with the ill-posed inverse problem associated with EIT. The structure of the system is illustrated in Fig. 5.

5.3 Determination of soluble sugar and starch contents

The sampled stem segments were washed with deionized water, oven dried at 80 °C for 48 h, and then kept in desiccators before use. Soluble sugar and starch contents were determined using the anthrone colorimetric method [33]. Eight samples from each replicate were used. The sample was ground into powder and 0.2 g of the powder was transferred into a 10 mL centrifuge tube. Then, 80% ethanol was added and the tube was incubated in a water bath at 80 °C. The extraction was performed three times by centrifugation. The supernatants of each extraction were combined in a volumetric flask and 80% ethanol was added to make the final volume of 25 mL. From this flask, exactly 0.8 mL of the solution was transferred into a 10 mL centrifuge tube that was then placed in a 100 °C water bath. The liquid was allowed to evaporate completely. The sugar in the centrifuge tube was completely dissolved in 5 mL water with the help of stirring. Finally, the solution was centrifuged, and the supernatant was removed and used for measuring.

To the precipitate in the tube, 2 mL water was added and the two were mixed by stirring. The tube was placed in boiling water for 15 min, and the precipitate formed a paste. After cooling on ice, 2 mL of 9.2 mol/L perchloric acid was added and the mixture was stirred well. After 15 min, 3 mL water was added, and the mixture was stirred well. The tube was then centrifuged for 10 min. The supernatant was poured into a 50 mL volumetric flask. To the precipitate in the tube, 2 mL of 4.6 mol/L perchloric acid was added and the mixture was stirred well. After 15 min, 3 mL of water was added, the mixture was stirred well, and then centrifuged for 10 min. This supernatant was also poured into the 50 mL volumetric flask. Finally, the precipitate was washed with 4 mL water and centrifuged. The centrifuged supernatant was combined with the previous supernatants collected in the 50 mL volumetric flask. Distilled water was added to make a final volume of 50 mL.

In a clean test tube, 1 mL water, and then 1 mL of extract (centrifuged supernatants collected in the 50 mL flask) were added. For the control, the test tube contained 2 mL water. Along the wall of the test tube, 5 mL 0.2% anthrone was slowly added, and the solution in the tube was mixed by shaking. The test tube was then incubated in an 80 °C water bath for 10 min to display color. After being cooled, the absorbance of the solution was measured at 620 nm. The soluble sugar and starch contents were calculated according to the following equations (1) and (2):

$$\text{Soluble sugar}\ (\%)=\frac{C\cdot n\cdot(V/\alpha)}{W\times 1000}\times 100\% \qquad (1)$$

$$\text{Starch}\ (\%)=\frac{C\cdot n\cdot(V/\alpha)\times 0.9}{W\times 1000}\times 100\% \qquad (2)$$

where C is the glucose content (μg) of the tested sample in the cuvette, which was read from a standard curve; V represents the total volume of extracts (mL); α represents the volume of extracts (mL) used in displaying color; represents the fold of dilution; is the dry weight of the sample (mg); and 0.9 is the glucose to starch conversion constant.

5.4 Statistical analysis

Microsoft Excel 2016 was used to remove anomalous data according to error theory. The curves of the reconstructed EIT boundary voltage values and the soluble sugar and starch contents changing with the sampling times were plotted using SigmaPlot V 10.0 (mean values were used in the figure). The correlation and variance of reconstructed EIT boundary voltage value, soluble sugar content, and starch content between the three floribunda cultivars and between the different sampling dates of each cultivar were analyzed using SPSS V 20.0 software. SPSS V 22.0 was used to establish the regression models for the average soluble sugar or starch content (dependent variable *y*) of the 'Red Cap' and 'Carefree Wonder' stems as a function of their corresponding reconstructed EIT boundary voltage values (independent variable *x*). The measured data for the cultivar 'Tender and Soft as Water' were used in statistical analysis and verification of the accuracy of the regression models.

6. Declarations

6.1 Ethics approval and consent to participate

Not applicable.

6.2 Consent for publication

Not applicable.

6.3 Availability of data and materials

The datasets generated during and/ or analyzed during the current study are not publicly available due to [REASON(S) WHY DATA ARE NOT PUBLIC] but are available from the corresponding author on reasonable request.

6.4 Competing interests

The authors declare that they have no competing interests.

6.5 Funding

This research was supported by grants from the National Natural Science Foundation of China (31272190 awarded to G.Z.), The Financial Aid Project for the Introduction of Overseas Students in Hebei Province (C201838) and Hebei Province Higher Education Science and Technology Research Project (QN2019090).

6.6 Author Contributions

In this paper, Ji Qian and Gang Zhang planned the project and was responsible for part of the manuscript writing and editing. Juan Zhou and Bao Di contributed to sample preparation and methodology, Yang Liu and Juan Zhou contributed to data analysis and interpretation of the results.

6.7 Acknowledgments

We wish to thank Dr Feng Fu and his research team members for their excellent technical assistance.

6.8 Authors' information

[1]College of Horticulture, Hebei Agriculture University, Baoding, Hebei 071000, China;

[2]College of Electrical and Mechanical Engineering, Hebei Agricultural University, Baoding, Hebei 071000, China;

[3] Department of Software Engineering, Hebei Software Institute, Baoding Hebei 071000, China; * Corresponding author;

[4]The author contributed equally to this work.

References

1. Irina M, Martin S, Joerg F. Carbon transitions from either Calvin cycle or transitory starch to heteroglycans as revealed by 14C-labeling experiments using protoplasts from Arabidopsis. Physiologia Plantarum. 2013;149:25–44. DOI:https://doi.org/10.1111/ppl.12033.
2. Alison MS, Mark S. Coordination of carbon supply and plant growth. Plant Cell Environ. 2007;30:1126–49. DOI:https://doi.org/10.1111/j.1365-3040. 01708. X.
3. Sala A, Piper F, Hoch G. Physiological mechanisms of drought-induced tree mortality are far from being resolved. New Phytol. 2010;186(2):274–81. DOI:https://doi.org/10.1111/j.1469-8137.2009.03167.x.
4. Chapin F, Schulze S, E, D., & Mooney H, A. The ecology and economics of storage in plants. Annu Rev Ecol Syst. 1990;21:423–47. DOI:https://doi.org/10.1146/annurev.es.21.110190.002231.

5. Wang S, Ding G, Lin YL, Ji SY, X., & Zhan H. Seasonal changes of endogenous soluble sugar and starch in different developmental stages of Fargesia yunnanensis. JOURNAL OF WOOD SCIENCE. 2016;62:1–11. DOI:https://doi.org/10.1007/s10086-015-1521-8.
6. Wei J, Wu C, Jiang Y, Y., & Wang HL. Sample Preparation for Determination of Soluble Sugar in Red Jujube Fruits by Anthrone Method. Food science. 2014;35:136–40. DOI:https://doi.org/10.7506/spkx1002-6630-201424026.
7. Zhang C, Liu F, Kong W, Cui W, He P, Y, D., & Zhou W, J. (2016). Estimation and Visualization of Soluble Sugar Content in Oilseed Rape Leaves Using Hyperspectral Imaging. Transactions of the ASABE 59. 1499–505. DOI:https://doi.org/10.13031/trans.59.10485.
8. Li Y, Mehta R, Messing J. A new high-throughput assay for determining soluble sugar in sorghum internode-extracted juice. Planta. 2018;248:785–93. DOI:https://doi.org/10.1007/s00425-018-2932-8.
9. Webster J, G. (1990). Electrical impedance tomography. Taylor and Francis Group.
10. Wi H, Sohal H, McEwan A, Woo L, E, J., & Oh T, I. Multi-frequency electrical impedance tomography system with automatic self-calibration for long-term monitoring. IEEE Trans Biomed Circuits Syst. 2014;8(1):119–28. DOI:https://doi.org/10.1109/TBCAS.2013.2256785.
11. 10.1007/978-81-322-1768-8$434
Bera T, K., & Nagaraju J. (2014). A labVIEW based data acquisition system for electrical impedance tomography (EIT). In: Proceedings of the 3rd international conference on soft computing for problem solving. Springer India, (a): 377–389. DOI: https://doi.org/ 10.1007/978-81-322-1768-8$434.
12. Bera T, Nagaraju K, J., & Lubineau G. (2016). Electrical impedance spectroscopy (EIS)-based evaluation of biological tissue phantoms to study multifrequency electrical impedance tomography (Mf-EIT) systems]. J Vis, 19(4): 691–713. DOI: https://doi.org/ 10.1007/s12650-016-0351-0.
13. Ando Y, Mizutani K, Wakatsuki N. (2014). Electrical impedance analysis of potato tissues during drying. Journal of food engineering, 121(Jan.): 24–31. DOI: https://doi.org/ 10.1016/j.jfoodeng.2013.08.008.
14. Kanti B, T. (2014). Bioelectrical Impedance Methods for Noninvasive Health Monitoring: A Review. Journal of Medical Engineering, 1–28. DOI: https://doi.org/ 10.1155/2014/381251.
15. Chen X, Tzu-Jen H, Jeffrey K, Gregory MA, James B, E, S., & David M, D. Multi-channel electrical impedance tomography for regional tissue hydration monitoring. Physiol Meas. 2014;35(6):1137–47. DOI:https://doi.org/10.1088/0967-3334/35/6/1137.
16. Bayford RH. (2006). BIOIMPEDANCE TOMOGRAPHY (ELECTRICAL IMPEDANCE TOMOGRAPHY). Annu Rev Biomed Eng, 8(1): 63–91. DOI: https://doi.org/ 10.1146/annurev.bioeng.8.061505.095716.
17. 10.1039/C2AN
Bayford R, Tizzard A (2012). Bioimpedance imaging: an overview of potential clinical applications. Analyst. 137(20): 4635–4643. DOI: https://doi.org/10.1039/C2ANCole 35874C, K, S., & Guttman R. M. (1942). Electric impedance of frog egg. Journal of General Physiology. 25(5): 765–775. DOI:

18. Weigand M, Kemna A. (2017). Multi-frequency electrical impedance tomography as a non-invasive tool to characterize and monitor crop root systems. Biogeosciences 14: 921–39. DOI: https: //doi.org/10.5194/bg-14-921-2017.
19. Mary B, Abdulsamad F, Saracco G, Peyras L, Vennetier M, Mériaux P, et al. (2017). Improvement of coarse root detection using time and frequency induced polarization: from laboratory to field experiments. Plant Soil 417: 243–59. DOI: https: //doi.org/10.1007/s1110 4-017-3255-4.
20. Martin T, Günther T. (2013). Complex resistivity tomography (CRT) for fungus detection on standing oak trees. Eur J For Res 132: 765–76. DOI: https: //doi.org/10.1007/s1034 2-013-0711-4.
21. Jiao M, Gong L, Qian RJ, J., et al. Frost Hardiness Assessment of Floribunda Roses by Means of Electrical Impedance Tomography. Scientia Agricultura Sinica. 2017;050(007):1302–16. (In Chinese).
22. Guyot A, Ostergaard K, Lenkopane T, M., et al. (2013). Using electrical resistivity tomography to differentiate sapwood from heartwood: application to conifers. Tree Physiol, 33(2): 187–94. DOI: https://doi.org/ 1 10.1093/treephys/tps128.
23. Cole K, S., & Guttman R, M. Electric impedance of frog egg. Journal of General Physiology. 1942;25(5):765–75. DOI:https://doi.org/10.1085/jgp.25.5.765.
24. Li M, Li Q, Mao JY, H, P., & Wu Y, Y. (2016). Diagnosis and detection of phosphorus nutrition level for Solanum lycopersicum based on electrical impedance spectroscopy. Biosys Eng, 143:108–18. DOI: https://doi.org/ 10.1016/j.biosystemseng.2016.01.005.
25. Liu H, Fu Y, Hu M, Yu DW, J., & Liu H. Effect of green, yellow and purple radiation on biomass, photosynthesis, morphology and soluble sugar content of leafy lettuce via spectral wavebands “knock out”. Scientia Horticulturae. 2018;236:10–7. DOI:https://doi.org/10.1016/j.scienta.2018.03.02.
26. Wei K, Ma L, Sun C, Liu K, Zhao Q, Sun N, Tu Y, K., & Pan L, Q. Relationship between optical properties and soluble sugar contents of apple flesh during storage. Postharvest Biology Technology. 2020;159:111021. DOI:https://doi.org/10.1016/j.postharvbio.2019.111021.
27. Wang J, Dong W, Jiang SZ, He YG, Liu HS, Lv T, M., & Ji S, J. Influence of long-term cold storage on phenylpropanoid and soluble sugarmetabolisms accompanied with peel browning of ‘Nanguo’ pears duringsubsequent shelf life. Scientia Horticulturae. 2020;260:108888. DOI:https://doi.org/10.1016/j.scienta.2019.108888.
28. Keys A, J., & Leegood R. C. Photosynthetic nitrogen assimilation and associated carbon and respiratory metabolism. Springer. DOI: https://doi.org/ 10.1007/0-306-48138-3.
29. Avi G, George A, Varatharajan V, Ian T, Jacob JKK, Kell M, Andreas B, Kim HH, Eric B. Influence of diurnal photosynthetic activity on the morphology, structure, and thermal properties of normal and waxy barley starch. International Journal of Biological Macromolecules. 2017;98:188–200. DOI:http://dx.doi.org/10.1016/j.ijbiomac.2017.01.118.
30. Run T, Fu H, G, R., & Fang W, H. The permeability biology of plant cell membrane was studied by electrical impedance spectroscopy. Guangdong agricultural science. 2013;5:142–5. 05.006.

31. Repo T, Zhang M, Ryyppö A, et al. (1994). Effects of freeze-thaw injury on parameters of distributed electrical circuits of stems and needles of Scots pine seedlings at different stages of acclimation. J Exp Bot, 45(6): 823–33. DOI: https://doi.org/ 10.1093/jxb/45.6.823.
32. X DONG, Z. (2008). Recent Progress and Challenges in the Study of Bioimpedance Imaging. Chinese Journal of Biomedical Engineering. 27(5): 641–3, 649. DOI:https://doi.org/10.3969/j.issn.0258-8021.2008.05.001.
33. Zhang G, Sun BB, Li Z, Di B, Xiang DY, Meng Y. Effects of soil temperature on bud break, shoot and needle growth, and frost hardiness in Pinus sylvestris var. mongolica saplings during dehardening. Acta Physiol Plant. 2017;39:169. DOI:https://doi.org/10.1007/s11738-017-2470-1.

Figures

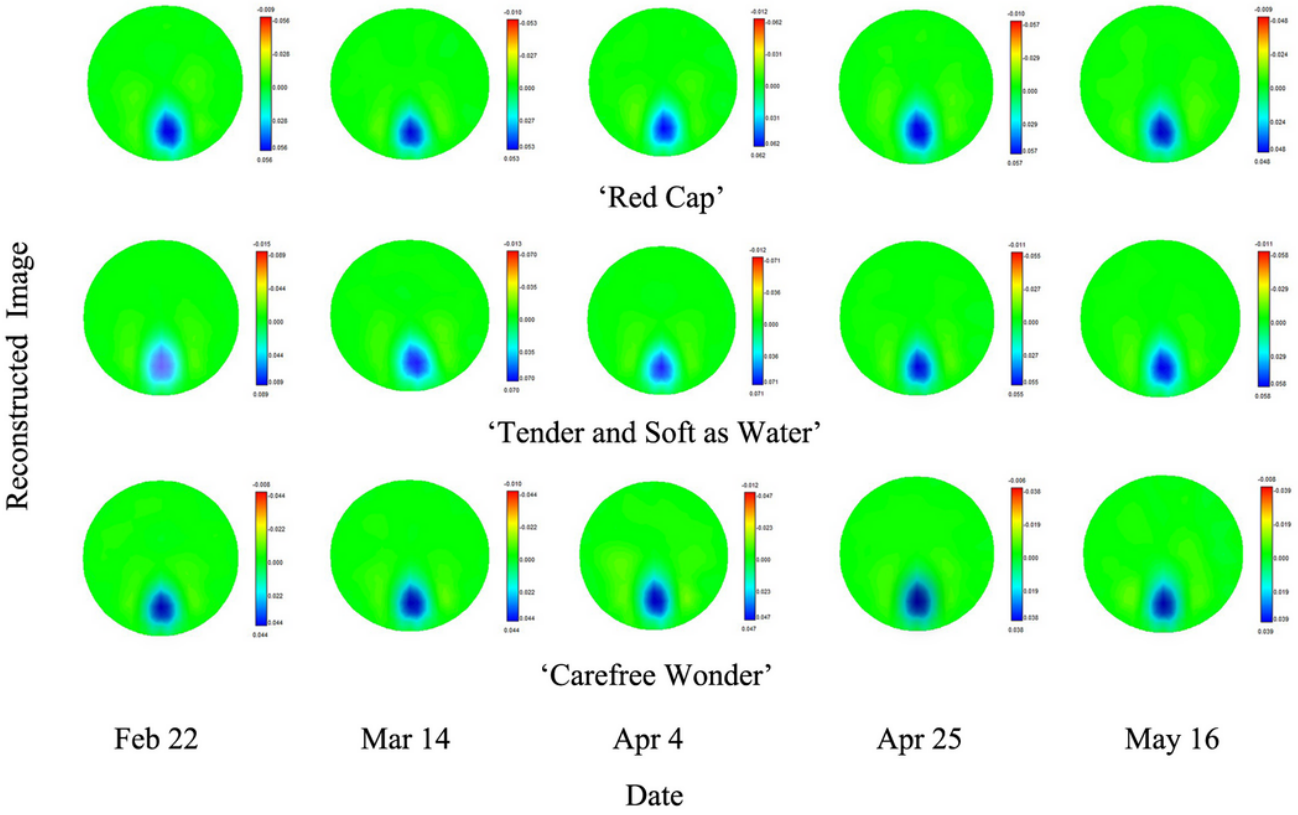

Figure 1

Electrical impedance tomography (EIT) images of the stems of three floribunda rose (Rosa hybrida) cultivars during the dehardening period

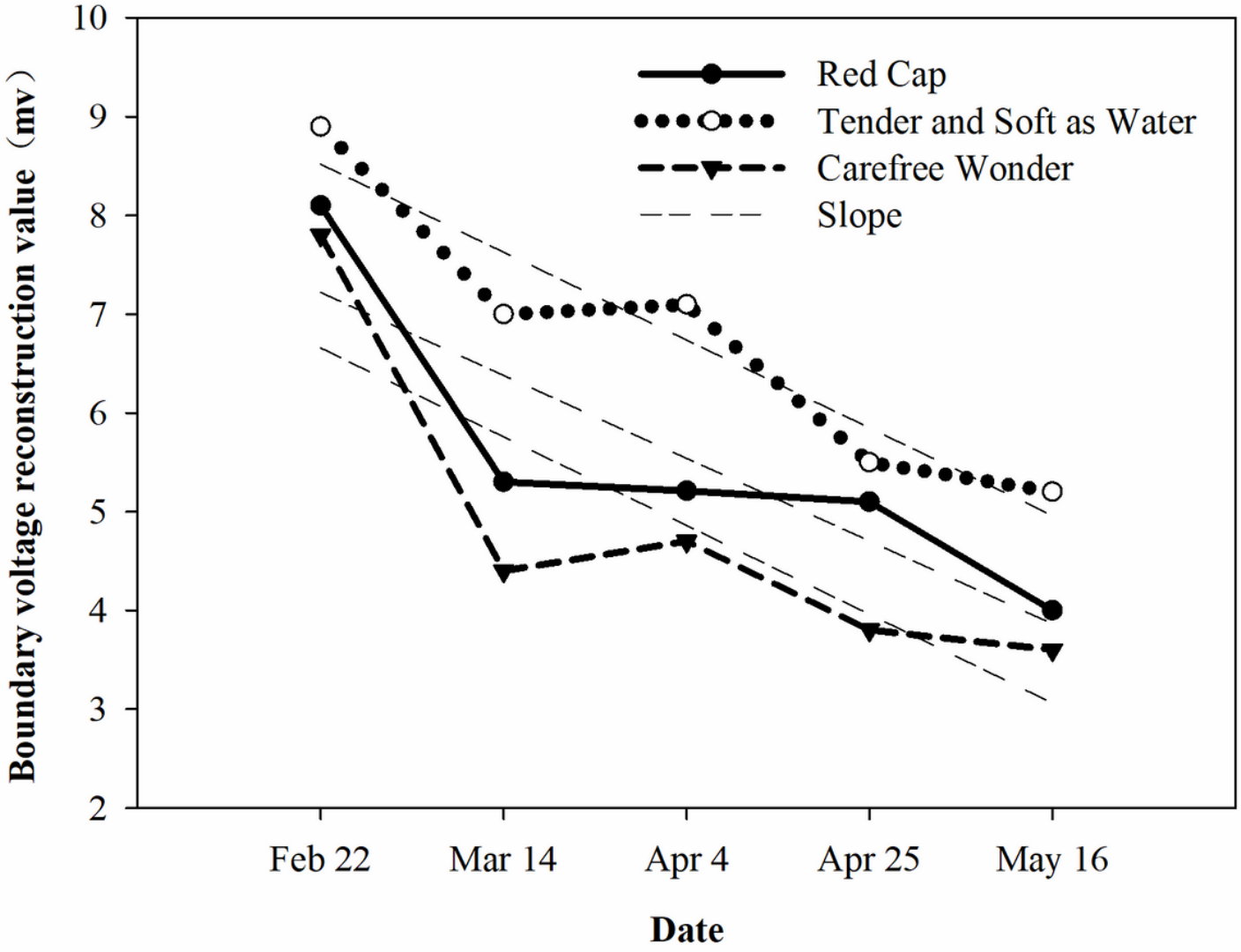

Figure 2

Reconstructed values of electrical impedance tomography (EIT) boundary voltages of the stems of three floribunda rose (Rosa hybrida) cultivars during the dehardening period

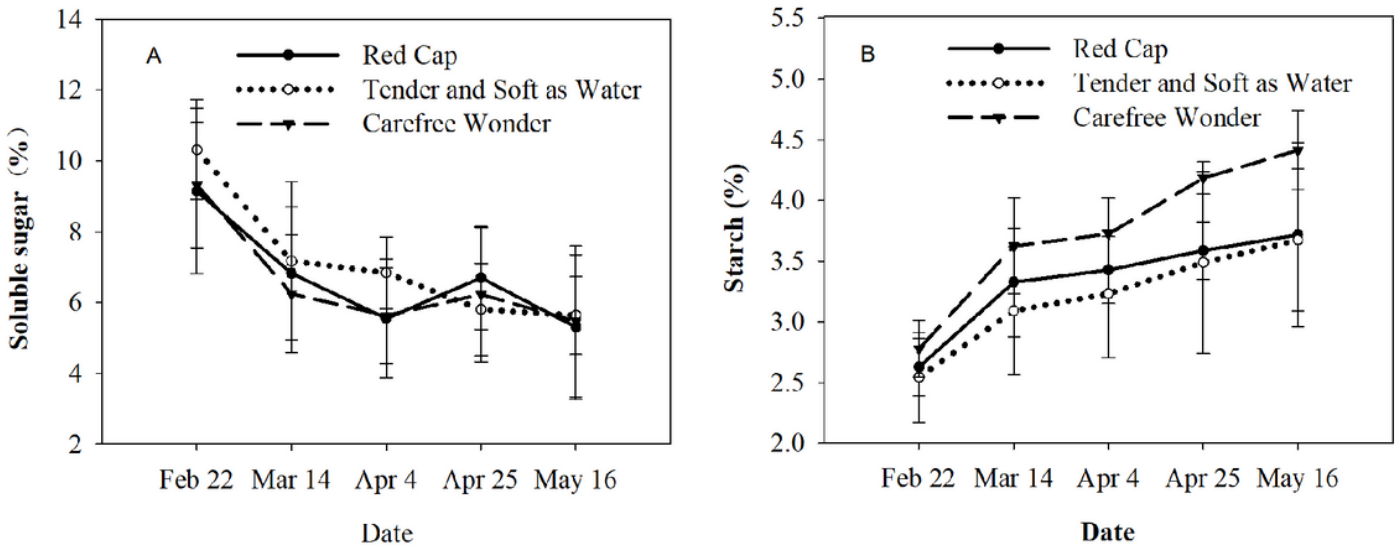

Figure 3

Soluble sugar content (A) and starch content (B) in the stems of three floribunda rose (Rosa hybrida) cultivars under natural conditions during the dehardening period

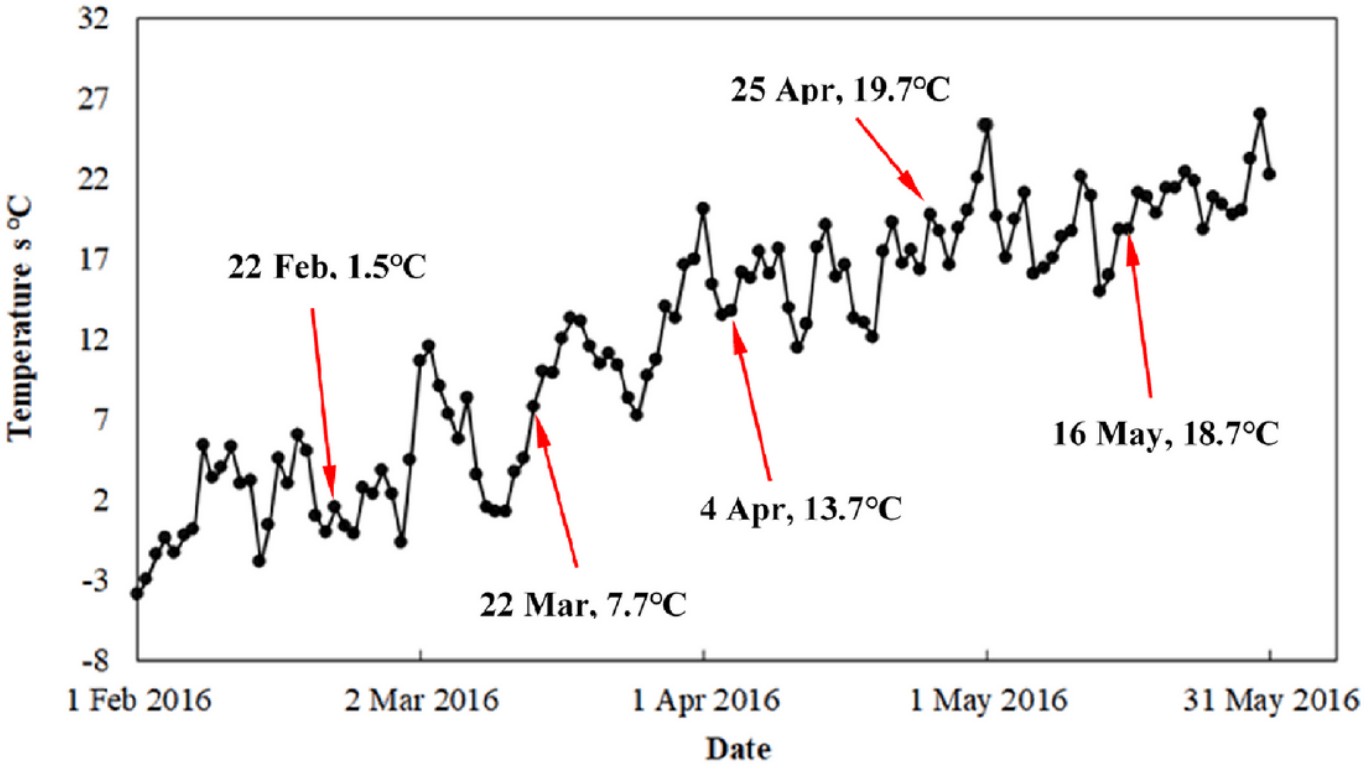

Figure 4

ng period

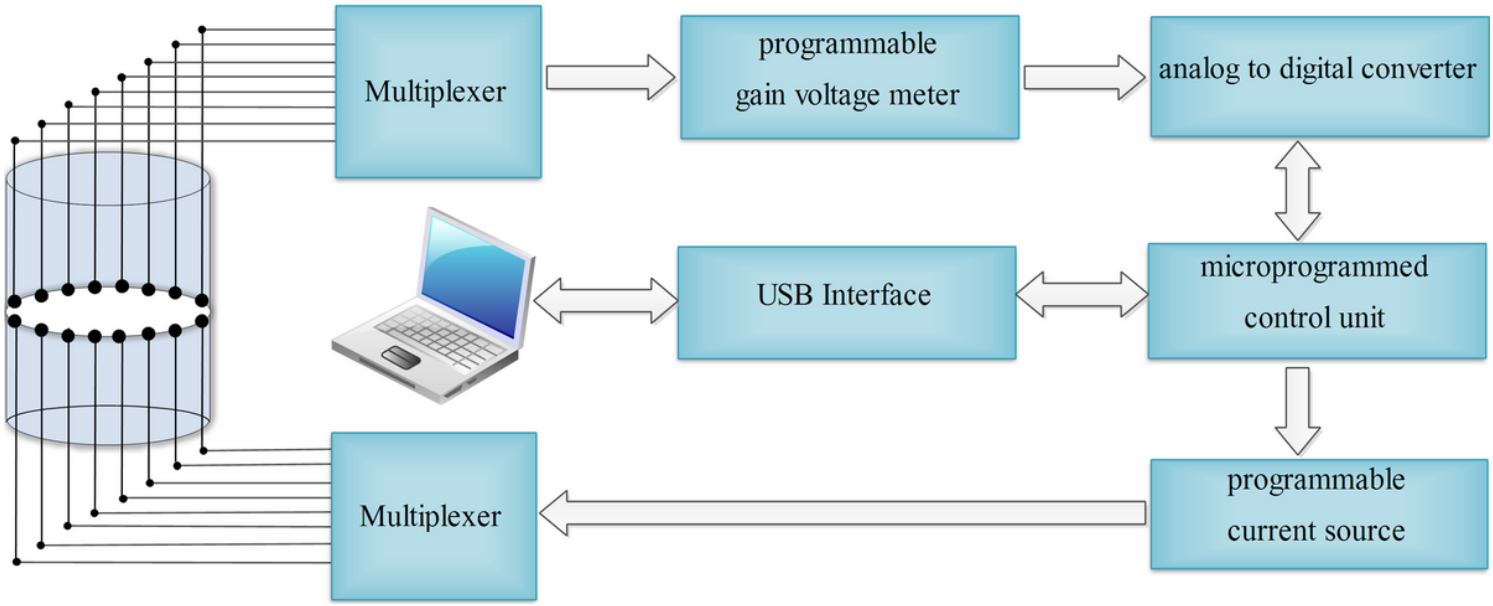

Figure 5

Diagram of the electrical impedance tomography (EIT) data acquisition system